Computational Process Control Compatible Dimensional Metrology Tool: Through-focus Scanning Optical Microscopy

Ravi Kiran Attota
Microsystem and Nanotechnology Division
National Institute of Standards and Technology
Gaithersburg, MD 20899, USA
Ravikiran.attota@nist.gov

Abstract—**Using only two derived numbers based on a reference library, this paper shows how through-focus scanning optical microscopy (TSOM) is compatible with computational process control (CPC) for the complete 3D shape process monitoring of nanoscale to microscale targets. This is demonstrated using three types of targets with widths (CDs) and depths ranging from 50 nm to 1.0 μm, and 70 nm to 20 μm, respectively. TSOM is a high-throughput, low-cost and in-line capable optical dimensional metrology method ideally suited for high-volume manufacturing (HVM), complementing other widely used metrology tools.**

Keywords—TSOM, process control, three-dimensional shape, optical microscope, through-focus, Computational Process Control

I. Introduction

As the applications of nanotechnology and micro-technology become widespread, usage of three-dimensional (3D) structures is increasing [1-10]. In addition, increased complexity and the resulting big data during manufacturing processes have resulted in a new paradigm: Computational Process Control (CPC) [11]. In the CPC environment, in-line metrology tools are highly desirable. Here, we present the through-focus scanning optical microscope (TSOM) as a dimensional metrology tool that is ideally compatible with CPC, and has many favorable attributes as a metrology and process control tool [12-21].

II. TSOM

TSOM is a method that collects and exploits the entire through-focus optical intensity information in 3-D space using a conventional optical microscope. Developments in image acquisition techniques have significantly reduced the acquisition time for a set of through-focus images so that it can be as fast as a single conventional microscope image, making TSOM suitable for HVM [22]. A vertical cross-section extracted from this 3D data results in a TSOM image. D-TSOM images are generated by taking a pixel-by-pixel difference between images of two separate targets. D-TSOM images can reveal sub-nanometer differences between nominally identical targets. The color (intensity) patterns of D-TSOM images are usually distinct for different types of parameter changes and serve as a "fingerprint" for different types of parameter variations, while remaining qualitatively similar for different magnitude changes in the same parameter. The magnitude of the optical content of D-TSOM images is proportional to the magnitude of the dimensional differences. The Optical Intensity Range (OIR, the difference between the maximum and the minimum optical intensity, multiplied by 100), provides a quantitative estimate of the difference between the two TSOM images. The utility of D-TSOM is that the color pattern of the D-TSOM image is an indicator of the difference in 3D shape, while the magnitude of the OIR scales the dimensional difference between the two targets.

III. Experiments

Fig.1

As a demonstration of the application of TSOM to high-aspect ratio (HAR) structures, in an SiO_2 layer on a 300 mm Si substrate with nominally 100 nm CD, 1100 nm depth, and 1000 nm pitch were studied, using a horizontal field-of-view (FOV) of 50 μm. A typical focused ion beam (FIB) cross-sectional view of the HAR target is shown Fig. 1. A mosaic of D-TSOM images obtained for the entire wafer (with central die as a reference target) is presented in Fig. 2(a). From this, four major types of D-TSOM image patterns (Fig. 2(b)) can be identified with their corresponding FIB cross-sectional profile differences as shown in Fig. 2(c).

IV. Process control results

If one considers the information available in Figs. 2(b) and 2(c) as a library, a simple process monitoring procedure can be proposed as shown in Figs. 3 and 4, based on the following rules selected for this demonstration. If the OIR of the D-TSOM image is more than 12, reject the target, as the dimensional differences are more than the tolerable limits. On the lower side, if the OIR of the D-TSOM image is less than 7, accept the target, as the dimensional differences are within the acceptable

level. If the OIR value is in between 7 and 12, accept the production target if the profiles are symmetric (T1 and T3) and reject if the profiles are asymmetric (T2 and T4). Selection of the rules depends on the desired outcome from the fabrication.

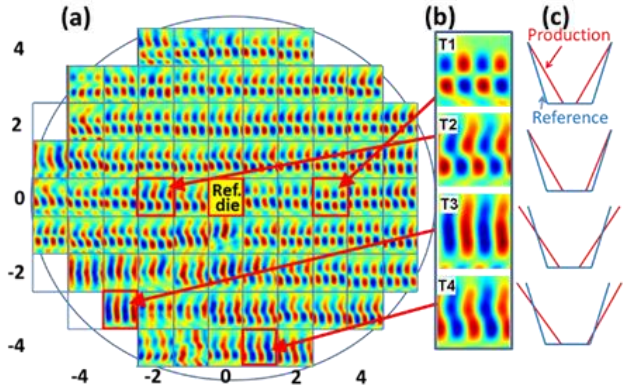

Fig. 2. (a) A mosaic of the D-TSOM images obtained by subtracting the TSOM image of the central reference target from the TSOM images of the targets in the other dies (with color scale bar set to automatic). (b) Four major types (T1, T2, T3 and T4) of D-TSOM image color patterns are identified. (c) *Schematic cross-sectional profile differences corresponding to (b) obtained from FIB cross-sectional analysis.* Nominal values: pitch = 1,000 nm, CD = 100 nm, and depth = 1100 nm. Illumination wavelength = 520 nm, numerical apertures (NA) = 0.75, illumination NA (INA) = 0.25.

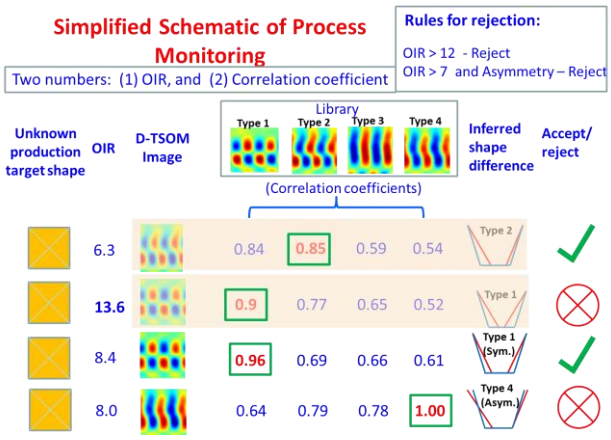

Fig. 3. Proposed TSOM-based automated 3-D-shape process control method. The selected test production targets are considered to have unknown 3-D-shape profile (column 1). Comparing the correlation coefficients between the D-TSOM images of the test targets and the library provides the best match (green boxes) from which the possible 3-D shape difference type can be inferred (column 8).

Fig. 3 demonstrates that based on the type of 3-D shape difference, and the magnitude of the dimensional difference, the process control decision of accept/reject can be made based solely on the two numbers: OIR and correlation coefficient with minimal or no human intervention to make it suitable for CPC. A library and a customized rule set must be created beforehand. Note that the process control decision is automatically made on the very optical tool during measurement using the previously mentioned numbers. This method nearly eliminates the need for post-processing.

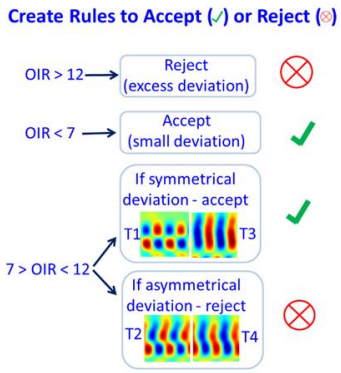

Fig. 4. This schematic shows that only two numbers are needed to accomplish the 3D-shape process control with TSOM. OIR to determine the magnitude of the dimensional deviation, and correlation coefficient to determine the 3D shape similarity.

A second example is shown in Fig. 5 for substantially smaller, isolated line targets with nominal sizes of 70 nm height and 50 nm width [17]. In this case also, since TSOM can identify different types of 3D-shape differences (down to 0.8 nm), the similar procedure presented above can be applied for process control.

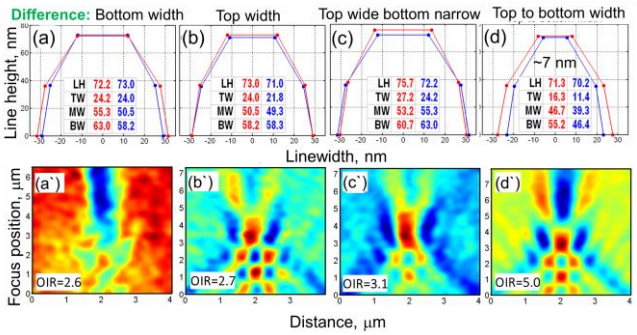

Fig. 5. Experimental 3D-shape analysis of isolated lines for process control. (a,b,c,d) CD-AFM-measured plots showing different types of 3D-shape differences. (a`,b`,c`,d`) are the corresponding D-TSOM images producing noticeably different color patterns. CD-AFM measured values of line height (LH), top width (TW), middle width (MW) and bottom width (BW, in nanometers) are shown in order for the pair of lines. Nominal height = 70 nm, and width = 50 nm.

A third example for a larger through-silicon via (TSV) target with a nominal diameter and depth of 1 µm and 20 µm respectively, is shown in Fig. 6. The similarity of the two D-TSOM images on the right indicates a similar pattern of dimensional differences. In this case also, the similar procedure presented above can be applied for process control using a library.

V. POTENTIAL APPLICATIONS

TSOM is a high-throughput, low-cost, nondestructive, robust, and easy-to-use 3D shape metrology method. It has 1 nm or better measurement resolution[14] for target sizes (depths/heights) ranging from sub-nanometer to over 100 um (over five orders of magnitude in size range). One of the unique

characteristics of the TSOM method is its ability to reduce or eliminate optical cross correlations between different parameters, resulting in reduced measurement uncertainty. All the targets within the field-of-view can be analyzed simultaneously, including isolated structures with random shapes, repeated and non-repeated structures, and a variety of target materials. TSOM complements other tools by filling in some gaps in capabilities.

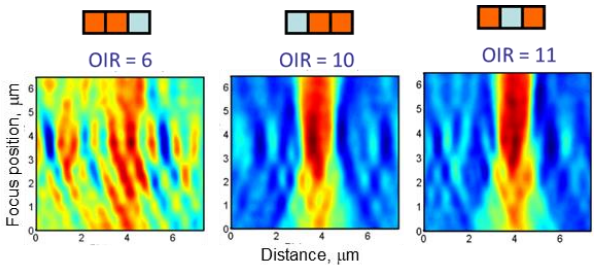

Fig. 6. Measured D-TSOM images representing the pairwise differences between TSOM images of three TSVs in three different dies. Nominal diameter = 1 μm, and depth = 20 μm.

TSOM has been successfully employed for many applications. Demonstrated applications of TSOM include critical dimension (linewidth), overlay (including over 10 um separation), patterned defect detection and analysis, FinFETs, nanoparticles (including soft-nanoparticles), photo-mask, thin-films (less than 0.5 nm to 10 nm) thickness, 2D materials, through-silicon vias (TSVs), high-aspect-ratio (HAR) targets, MEMS/NEMS devices, micro/nanofluidic channels, flexible electronics and micro-resonators/frequency combs. Other potential applications include three-dimensional shape process monitoring of self-assembled nanostructures, waveguides, and nanoimprint targets. Numerous industries benefit from the TSOM method —such as the semiconductor industry, flexible electronics, quantum science, photovoltaics, display, nanotechnology, MEMS, NEMS, biotechnology, data storage, and photonics.

VI. SUMMARY

Here we have briefly presented potential applications of TSOM using a reference library. TSOM could fill some gaps by satisfying the HVM metrology needs of 3-D structures for which 3-D shape process control/monitoring is needed, complementing other widely used metrology tools. We also show that TSOM as presented here has a high compatibility with computational process control.

ACKNOWLEDGEMENTS

The author would like to thank and acknowledge the contributions made by Hyeonggon Kang, Keana Scott, Richard Allen, Andras E. Vladar, Benjamin Bunday, Emil Agocs and John Kramar.

REFERENCES

1. M. H. Postek, Robert, "Instrumentation and metrology for nanotechnology," 2004).
2. G. B. Picotto, L. Koenders, and G. Wilkening, "Nanoscale metrology," Measurement Science and Technology **20**, 080101 (2009).
3. R. K. Leach, R. Boyd, T. Burke, H. U. Danzebrink, K. Dirscherl, T. Dziomba, M. Gee, L. Koenders, V. Morazzani, A. Pidduck, D. Roy, W. E. S. Unger, and A. Yacoot, "The European nanometrology landscape," Nanotechnology **22**(2011).
4. G. Häusler and S. Ettl, "Limitations of Optical 3D Sensors," in *Optical Measurement of Surface Topography*, R. Leach, ed. (Springer Berlin Heidelberg, 2011), pp. 23-48.
5. X. Zhang, H. Zhou, Z. Ge, A. Vaid, D. Konduparthi, C. Osorio, S. Ventola, R. Meir, O. Shoval, R. Kris, O. Adan, and M. Bar-Zvi, "Addressing FinFET metrology challenges in 1× node using tilt-beam critical dimension scanning electron microscope," MOEMS **13**, 041407-041407 (2014).
6. I. Schulmeyer, L. Lechner, A. Gu, R. Estrada, D. Stewart, L. Stern, S. McVey, B. Goetze, U. Mantz, and R. Jammy, "Advanced metrology and inspection solutions for a 3D world," in *2016 International Symposium on VLSI Technology, Systems and Application (VLSI-TSA)*, 2016), 1-2.
7. A. Arceo, B. Bunday, A. Cordes, and V. Vartanian, "Evolution or revolution: the path for metrology beyond the 22nm node," Solid State Technol **55**, 15-19 (2012).
8. T. F. Crimmins, "Defect metrology challenges at the 11-nm node and beyond," in 2010), 76380H-76380H-76312.
9. K. Takamasu, Y. Iwaki, S. Takahashi, H. Kawada, M. Ikota, G. F. Lorusso, and N. Horiguchi, "3D-profile measurement of advanced semiconductor features by reference metrology," in 2016), 97781T-97781T-97788.
10. R. Attota, R. Silver, and B. M. Barnes, "Optical through-focus technique that differentiates small changes in line width, line height and sidewall angle for CD, overlay, and defect metrology applications," Proc. SPIE **6922**, 69220E (2008).
11. D. Lammers, "COMPUTATIONAL PROCESS CONTROL SOLUTIONS TO SERVICE FABS IN CHINA" (2018), retrieved http://www.appliedmaterials.com/nanochip/nanochip-fab-solutions/march-2018/computational-process-control-solutions-to-service-fabs-in-china.
12. R. Attota, T. A. Germer, and R. M. Silver, "Through-focus scanning-optical-microscope imaging method for nanoscale dimensional analysis," Opt Lett **33**, 1990-1992 (2008).
13. R. Attota and R. Silver, "Nanometrology using a through-focus scanning optical microscopy method," Meas Sci Technol **22**(2011).
14. R. Attota, B. Bunday, and V. Vartanian, "Critical dimension metrology by through-focus scanning optical microscopy beyond the 22 nm node," Appl Phys Lett **102**(2013).
15. M. Ryabko, S. Koptyaev, A. Shcherbakov, A. Lantsov, and S. Y. Oh, "Motion-free all optical inspection system for nanoscale topology control," Opt Express **22**, 14958-14963 (2014).
16. S. Han, T. Yoshizawa, S. Zhang, J. H. Lee, J. H. Park, D. Jeong, E. J. Shin, and C. Park, "Tip/tilt-compensated through-focus scanning optical microscopy," Proc. of SPIE **10023**, 100230P (2016).
17. R. Attota and R. G. Dixson, "Resolving three-dimensional shape of sub-50 nm wide lines with nanometer-scale sensitivity using conventional optical microscopes," Appl Phys Lett **105,** 043101, (2014).
18. R. Attota, R. G. Dixson, J. A. Kramar, J. E. Potzick, A. E. Vladar, B. Bunday, E. Novak, and A. Rudack, "TSOM Method for Semiconductor Metrology," Proc. SPIE **7971**, 79710T (2011).
19. A. Arceo, B. Bunday, V. Vartanian, and R. Attota, "Patterned Defect & CD Metrology by TSOM Beyond the 22 nm Node," Proc Spie **8324**(2012).
20. S.-w. Park, G. Park, Y. Kim, J. H. Cho, J. Lee, and H. Kim, "Through-focus scanning optical microscopy with the Fourier modal method," Opt Express **26**, 11649-11657 (2018).
21. S. I. Association, "The International Technology Roadmap for Semiconductors (ITRS) " (Semiconductor Industry Association, San Jose, 2016).
22. R. Attota, "Through-focus or volumetric type of optical imaging methods: a review," J Biomed Opt **23**, 19100-19114 (2018).
23. R. K. Attota, H. Kang, K. Scott, R. Allen, A. E. Vladar, and B. Bunday, "Nondestructive shape process monitoring of three-dimensional, high-aspect-ratio targets using through-focus scanning optical microscopy," Measurement Science and Technology **29**, 125007 (2018).